

Divergence in Møller–Plesset theory: A simple explanation based on a two-state model

Cite as: J. Chem. Phys. **112**, 9736 (2000); <https://doi.org/10.1063/1.481611>

Submitted: 08 December 1999 . Accepted: 15 March 2000 . Published Online: 31 May 2000

Jeppe Olsen, Poul Jørgensen, Trygve Helgaker, and Ove Christiansen



View Online



Export Citation

ARTICLES YOU MAY BE INTERESTED IN

[Surprising cases of divergent behavior in Møller–Plesset perturbation theory](#)

The Journal of Chemical Physics **105**, 5082 (1996); <https://doi.org/10.1063/1.472352>

[Why does MP2 work?](#)

The Journal of Chemical Physics **145**, 184101 (2016); <https://doi.org/10.1063/1.4966689>

[Is Møller–Plesset perturbation theory a convergent ab initio method?](#)

The Journal of Chemical Physics **112**, 9213 (2000); <https://doi.org/10.1063/1.481764>

PHYSICS TODAY
WHITEPAPERS

ADVANCED LIGHT CURE ADHESIVES

Take a closer look at what these environmentally friendly adhesive systems can do

READ NOW

PRESENTED BY
MASTERBOND
ADHESIVES • SEALANTS • COATINGS



Divergence in Møller–Plesset theory: A simple explanation based on a two-state model

Jeppe Olsen and Poul Jørgensen^{a)}

Department of Chemistry, University of Aarhus, DK-8000 Aarhus, Denmark

Trygve Helgaker^{b)}

Department of Chemistry, University of Cambridge, Lensfield Road, CB2 1EW, United Kingdom

Ove Christiansen

Chemical Centre, University of Lund, P.O.B. 124, S-22100 Lund, Sweden

(Received 8 December 1999; accepted 15 March 2000)

The convergence of the Møller–Plesset expansion is examined for Ne, F⁻, CH₂, and HF and analyzed by means of a simple two-state model. For all systems, increasing diffuseness of the basis introduces highly excited diffuse back-door intruder states, resulting in an alternating, ultimately divergent expansion. For F⁻, the divergence begins already at third order; for the remaining systems, it begins later. For CH₂, the low-lying doubly excited state leads to a monotonic, slowly decreasing series at lower orders; for the stretched HF molecule, the low-lying doubly excited states lead to a slowly undulating series at lower orders. Although the divergence of the Møller–Plesset series does not invalidate the use of the second-order expansion, it questions the use of higher-order Møller–Plesset expansions in quantum-chemical studies. © 2000 American Institute of Physics. [S0021-9606(00)30122-2]

I. INTRODUCTION

Quantum-chemical calculations are nowadays widely used to analyze, interpret, and predict experimental data. The development of efficient schemes and programs for Møller–Plesset (MP) perturbation theory¹ has been important for obtaining this status. The second-order version of MP theory (MP2) is presently perhaps the most widely used correlated *ab initio* model. Third- (MP3) and fourth- (MP4) order methods have also been extensively used and have been implemented in a number of standard quantum-chemical programs. Recently, MP5 and MP6 has also been efficiently implemented.²

From a huge body of calculations, it is now well established that the MP2 method in most cases gives a significant and cost-effective improvement on the uncorrelated Hartree–Fock (HF) method. However, it is also known that the MP series may not converge when the HF state is a poor approximation to the exact wave function.³ Furthermore, recent investigations have brought into question the reliability of higher-order MP theory also for molecules without near-degenerencies.⁴ The surprising aspect of the newly reported divergences was that they occur for systems such as the neon atom and the equilibrium water molecule, which traditionally have been considered as well-behaved systems for MP theory. Indeed, the divergences appear to be inherent to the MP series, arising from spatially extended intruder states that are highly excited relative to the ground-state reference wave function.⁵ Such states occur whenever the one-

electron basis is sufficiently flexible to describe the diffuse intruder states. For the above-mentioned systems, the MP series converges in small basis sets without diffuse functions^{6,7} but diverges when these sets are augmented with diffuse functions.⁴

The divergence of the MP series has conceptual as well as practical ramifications. The conceptual consequences relate to the fact that MP theory can no longer be considered to provide a hierarchy of methods where an improved accuracy is obtained at higher levels. The practical consequences may be illustrated by a couple of examples. For F⁻ in the aug-cc-pVDZ basis, the smallest error in the MP series occurs at the MP2 level. Since aug-cc-pVDZ is the smallest basis that can properly describe this anion, it becomes altogether questionable to apply Møller–Plesset theory beyond second order. A similar conclusion was drawn in an interesting study where extrapolations to the basis-set limit were carried out for MP2, MP3, MP4, and MP5 for various properties of small molecules.⁸ For equilibrium geometries and vibrational frequencies, the MP2 results were often the most accurate ones, with a deterioration in the performance of the MP methods when the basis set was extended. This is of course a very undesirable feature that prevents the use of MP theory to obtain accurate results. In Ref. 8, it was stated that the reason for this undesirable behavior has yet to be uncovered.

In this work, we extend our previous analysis of the divergence in the MP series for Ne,⁵ discussing the divergences of the MP series for Ne, F⁻, CH₂, and HF and use a simple mathematical model to show how the divergences can be given a simple physical interpretation by means of a two-state model. For other examples of perturbational analysis in terms of a two-state models see Refs. 9 and 10 and references therein. In particular, we clarify the nature of the in-

^{a)}Electronic mail: pou@kemi.aau.dk

^{b)}Permanent address: Department of Chemistry, University of Oslo, P.O.B. 1033 Blindern, N-0315 Oslo, Norway.

truders responsible for the observed divergences and explain why such divergences will nearly always occur in a sufficiently diffuse basis set.

The convergence behavior of the CH₂ molecule is examined in terms of the near-degeneracy of the ground state and a low-lying doubly excited state. For the Ne atom, the MP divergence is analyzed as a prototypical example of a system with a back-door intruder, demonstrating that the divergence also persists for larger basis sets. For the HF molecule, we present a detailed convergence analysis, both at the equilibrium geometry and at a stretched geometry, discussing the different characters of the intruder states in these cases.

II. CONVERGENCE IN PERTURBATION THEORY

A. General convergence criteria

General criteria for the convergence of perturbation expansions in a finite-dimensional space have been derived by Kato.¹¹ Here we give a simplified discussion of the theory as relevant in this context.¹² We consider the partitioned Hamiltonian,

$$\mathbf{H}(z) = \mathbf{H}_0 + z\mathbf{U}, \quad (1)$$

where z is a complex *strength parameter*. The zeroth-order problem is represented by $z=0$ and $z=1$ represents the physical problem. The eigenvalue equation,

$$\mathbf{H}(z)\mathbf{C}_k(z) = E_k(z)\mathbf{C}_k(z), \quad (2)$$

defines the energy function $E_k(z)$. The expansion of $E_k(z)$ in z ,

$$E_k(z) = \sum_{n=0}^{\infty} E_k^{(n)} z^n, \quad (3)$$

has a finite *radius of convergence* R such that $E_k(z)$ converges for $|z| < R$ and diverges for $|z| > R$. Our perturbation expansion, Eq. (3), thus converges if $R > 1$ and diverges if $R < 1$.

A *point of degeneracy* for $E_k(z)$ is defined as a point ζ , where the state k is degenerate with another state l : $E_k(\zeta) = E_l(\zeta) = E_{kl}$. It is easy to show that, for real and symmetric matrices \mathbf{H}_0 and \mathbf{U} , such points always occur in conjugate pairs (ζ, ζ^*) . The location of the points of degeneracy in the complex plane is important since the radius of convergence is the distance from the expansion point $(0,0)$ to the nearest point of degeneracy of $E_k(z)$. Degeneracies of $E_k(z)$ in the complex plane within the unit circle therefore lead to a divergent Møller–Plesset expansion.

A state that becomes degenerate with the reference state at a point ζ inside the unit circle $|\zeta| < 1$ is called an *intruder state*. In this terminology, the requirement for convergence is simply the absence of intruder states. An intruder state with $\Re(\zeta) > 0$ is called a *front-door intruder*; conversely, a *back-door intruder* has $\Re(\zeta) < 0$.

From this discussion, it follows that the convergence of the MP expansion does not depend directly on the agreement of \mathbf{H} and \mathbf{H}_0 in terms of some matrix norm; rather, it depends on our ability to select a zeroth-order matrix \mathbf{H}_0 such that the eigenvalues of $\mathbf{H}_0 + z\mathbf{U}$ are nondegenerate for any complex strength parameter inside the unit circle.

In practice, it may not be possible to carry out an exhaustive search for degeneracies inside the unit circle. However, since avoided crossings on the real axis are indicative of degeneracies in the complex plane, much useful information may be obtained by investigating the energies for real z .^{13,14} Of course, the identification of an avoided crossing on the real axis is not sufficient to establish divergence since the degeneracy may occur outside the unit circle. However, as we shall see in the next section, by projecting the zeroth-order Hamiltonian and the perturbation operator onto a two-dimensional space spanned by the roots of $\mathbf{H}(z)$ for real z , we may estimate the real and imaginary components of the point of degeneracy and thereby obtain an indication whether the expansion is convergent or divergent.

When the number of parameters [i.e., the dimension of $\mathbf{H}(z)$] is large, a complete scan of the spectrum of $\mathbf{H}(z)$ for real z is a difficult computational task. A simpler method is obtained by performing the scan in a subspace of the correction vectors generated in a given perturbation expansion. For example, if the energy is calculated to order $2n+1$, the wave-function corrections are determined to order n and the subspace Hamiltonian is set up in this $(n+1)$ -dimensional space. Since, in standard perturbation calculations, the matrix elements of the perturbation operator as well as the overlap of the perturbation vectors are already calculated in this subspace, we must calculate, in addition, only the matrix elements of the zeroth-order Hamiltonian in order to perform a scan. Such a restricted scan can therefore be appended to standard perturbation calculations at little cost. As we shall see, restricted scans provide a simple way of studying the occurrence of intruder states in perturbation theory.

B. A two-state model

It is often useful to analyze the convergence behavior of perturbation expansions by means of a two-state model.^{9,10} Here we describe a two-state model that will prove particularly useful for discussing divergences in MP theory.

We consider the two-state problem given by the Hamiltonian matrix,

$$\mathbf{H} = \begin{pmatrix} \alpha & \delta \\ \delta & \beta \end{pmatrix}, \quad (4)$$

where all parameters are real, and we assume that $\beta > \alpha$. We partition the Hamiltonian matrix Eq. (4) into a zeroth-order part and a perturbation part,

$$\mathbf{H}_0 = \begin{pmatrix} \alpha + \alpha_s & 0 \\ 0 & \beta + \beta_s \end{pmatrix}, \quad (5)$$

$$\mathbf{U} = \begin{pmatrix} -\alpha_s & \delta \\ \delta & -\beta_s \end{pmatrix}, \quad (6)$$

where α_s and β_s are the *level-shift parameters*, describing the *level shifts* of the zeroth-order Hamiltonian. The level shifts do not appear in the physical Hamiltonian \mathbf{H} and therefore do not affect the eigenvalues of \mathbf{H} . However, they determine the dependence of $\mathbf{H}(z)$ and z and thus the perturbation series and its convergence properties.

The eigenvalues of $\mathbf{H}_0 + z\mathbf{U}$ are readily obtained as

$$E_{\pm}(z) = \frac{\alpha + \beta + (1-z)(\gamma + 2\alpha_s)}{2} \pm \frac{\sqrt{[\epsilon + (1-z)\gamma]^2 + 4\delta^2 z^2}}{2}, \quad (7)$$

where we have introduced the *energy-gap parameter*,

$$\epsilon = \beta - \alpha, \quad (8)$$

and the *gap-shift parameter*,

$$\gamma = \beta_s - \alpha_s. \quad (9)$$

For $z=1$, Eq. (7) reduces to the physical energies—that is, to the eigenvalues of $\mathbf{H}(1)$. For the expansion of the lowest energy, the energy corrections become

$$E^{(0)} = \min(\alpha + \alpha_s, \beta + \beta_s), \quad (10)$$

$$E^{(1)} = \begin{cases} -\alpha_s: & E^{(0)} = \alpha + \alpha_s, \\ -\beta_s: & E^{(0)} = \beta + \beta_s, \end{cases} \quad (11)$$

$$E^{(n)} = \frac{|\epsilon + \gamma|(n-2)!}{(\epsilon + \gamma)^n} \times \sum_{k=1}^{[n/2]} \frac{(-1)^k}{(n-2k)!k!(k-1)!} \gamma^{n-2k} \delta^{2k}, \quad n \geq 2, \quad (12)$$

where $[n/2]$ is the largest integer smaller than or equal to $n/2$. From Eq. (12), we see that the higher-order corrections depend on the level shifts α_s and β_s only through the gap-shift parameter γ . Moreover, even though the zeroth- and first-order energies, Eqs. (10) and (11), depend separately on the level shift α_s , their sum is constant. We shall therefore in the following analyze the convergence behavior of the perturbation expansion as functions of the three parameters ϵ , γ , and δ . Note that $\epsilon > 0$, γ can be both negative, positive, or zero, and the sign of δ is related to the relative phases of the two states. The case $\delta=0$ is trivial and we consider only $|\delta| > 0$.

Instead of examining the convergence of the explicit form of the energy corrections in Eq. (12), we return to the analytical expressions for the eigenvalues, Eq. (7). To locate the points of degeneracy for $E_{\pm}(z)$, we set $E_+(\zeta_{\pm}) = E_-(\zeta_{\pm})$ and obtain the conjugate solutions

$$\zeta_{\pm} = \frac{\epsilon + \gamma}{4\delta^2 + \gamma^2} (\gamma \pm 2\delta i). \quad (13)$$

Note that, whereas the unshifted problem ($\gamma=0$) has pure imaginary points of degeneracy,

$$\zeta_{\pm}(\gamma=0) = \pm i \frac{\epsilon}{2\delta}, \quad (14)$$

the shifted problem has complex points of degeneracy. In the two-dimensional case, these points may never become real but, for large gap-shifts and small couplings, they may come arbitrarily close to the real axis.

For $|\zeta_{\pm}| < 1$, the points of degeneracy become intruders. Equation (13) shows that back-door intruders may occur for gap shifts in the interval $-\epsilon < \gamma < 0$ and that other gap shifts give rise to front-door intruders. For large (positive or nega-

tive) gap shifts, the points of degeneracy approach $z=1$ with vanishing imaginary components. For $\gamma = -\epsilon$, the zeroth-order Hamiltonian becomes degenerate and the radius of convergence is zero. Conversely, for $\gamma = 4\delta^2/\epsilon$, the point of degeneracy is located as far away from zero as possible, presumably leading to the most rapidly convergent series. When $|\zeta_{\pm}| > 1$, the series in Eqs. (10)–(12) is convergent. Thus, the series is convergent for

$$\frac{(\epsilon + \gamma)^2}{4\delta^2 + \gamma^2} > 1 \quad (15)$$

or

$$\frac{\epsilon^2}{4} \left(1 + \frac{2\gamma}{\epsilon} \right) > \delta^2. \quad (16)$$

Solving Eq. (16) for δ , we obtain for $2\gamma/\epsilon > -1$,

$$|\delta| < \frac{\epsilon}{2} \sqrt{1 + \frac{2\gamma}{\epsilon}}, \quad (17)$$

which should be compared with the convergence criterion $|\delta| < \epsilon/2$ for the unshifted problem ($\gamma=0$). For $2\gamma/\epsilon < -1$, the series diverges. Solving Eq. (15) for γ , we obtain the convergence criterion

$$\gamma > \frac{4\delta^2 - \epsilon^2}{2\epsilon}. \quad (18)$$

Thus, for any energy gap ϵ and any coupling δ , there exists a gap shift γ for which the expansion converges. The convergence of the perturbation expansion is summarized in Table I.

As we usually can locate only the avoided crossings (rather than the points of degeneracy) of the matrix $\mathbf{H}(z)$, it is important to determine the relation between the positions of the avoided crossings and the associated points of degeneracy. In the two-state model, there is only one avoided crossing, which is located by minimizing the difference between the two energies in Eq. (7) for real z . It turns out that the avoided crossing coincides with the real part of the positions of the points of degeneracy:

$$z_{\min} = \Re(\zeta_{\pm}) = \frac{\epsilon + \gamma}{4\delta^2 + \gamma^2} \gamma. \quad (19)$$

The corresponding energy gap is given by

$$\Delta E(z_{\min}) = 2 \frac{|(\epsilon + \gamma)\delta|}{\sqrt{4\delta^2 + \gamma^2}}. \quad (20)$$

For small coupling δ , the avoided crossing becomes pronounced, with the two curves coming very close at z_{\min} . Conversely, if δ and $\epsilon + \gamma$ are both numerically large, the two curves are well separated at z_{\min} , indicating that the points of degeneracy are located far from the real axis and that it may be difficult to give an accurate estimate of the location of the avoided crossing.

In the case where the coupling is small relative to the gap shift $|\delta| \ll |\gamma|$, the expression for the energy corrections Eq. (12) may be simplified as follows:

TABLE I. Convergence behavior of the perturbation expansion of the two-state problem for a given $\epsilon > 0$ and various values of γ and $|\delta| > 0$.

γ	Convergence info.	Degeneracy information
$\gamma < -\epsilon$	Divergent	$\Re(\zeta_{\pm}) > 0$
$\gamma = -\epsilon$	Divergent	$\zeta_{\pm} = 0$
$-\epsilon < \gamma < -\frac{\epsilon}{2}$	Divergent	$\Re(\zeta_{\pm}) < 0$
$\gamma = -\frac{\epsilon}{2}$	Divergent for $ \delta > 0$	$\Re(\zeta_{\pm}) < 0$
$-\frac{\epsilon}{2} < \gamma < 0$	Convergent for $ \delta < \frac{\epsilon}{2} \sqrt{1 + \frac{2\gamma}{\epsilon}}$	$\Re(\zeta_{\pm}) < 0$
	Divergent for $ \delta > \frac{\epsilon}{2} \sqrt{1 + \frac{2\gamma}{\epsilon}}$	$\Re(\zeta_{\pm}) < 0$
$\gamma = 0$	Convergent for $ \delta < \frac{\epsilon}{2}$	$\Re(\zeta_{\pm}) = 0$
	Divergent for $ \delta > \frac{\epsilon}{2}$	$\Re(\zeta_{\pm}) = 0$
$0 < \gamma < \frac{4\delta^2 - \epsilon^2}{2\epsilon}$	Convergent for $ \delta < \frac{\epsilon}{2} \sqrt{1 + \frac{2\gamma}{\epsilon}}$	$\Re(\zeta_{\pm}) > 0$
	Divergent for $ \delta > \frac{\epsilon}{2} \sqrt{1 + \frac{2\gamma}{\epsilon}}$	$\Re(\zeta_{\pm}) > 0$
$\frac{4\delta^2 - \epsilon^2}{2\epsilon} < \gamma$	Convergent	$\Re(\zeta_{\pm}) > 0$

$$E^{(n)} = -\frac{\gamma^{n-2} \delta^2}{(\epsilon + \gamma)^{n-1}}. \quad (21)$$

When the gap shift is positive (as for usual front-door intruders), this expression shows that all energy corrections are negative. For a negative gap shift that does not change the order of the zeroth-order states (as for typical back-door intruders), this expression predicts an alternating series with negative even-order corrections and positive odd-order corrections. In the same limit $|\delta| \ll |\gamma|$, the ratio between two consecutive energy corrections is given by

$$\frac{E^{(n)}}{E^{(n-1)}} = \frac{\gamma}{\epsilon + \gamma}, \quad (22)$$

showing that the relative change of the energy corrections depends only on the ratio of the gap shift γ to the zeroth-order energy gap $\epsilon + \gamma$. When the numerical value of the gap shift γ is significantly larger than the energy gap ϵ , a slow convergence is thus obtained.

The model, Eq. (21), cannot explain situations where the energy corrections first decrease in magnitude and then increase (asymptotic convergence). Such a behavior can be obtained in the two-state model but occurs as a result of a complicated interplay among the different contributions to Eq. (12) and requires more than a single term to be retained in the expression for the energy correction.

III. EXAMPLES OF MØLLER–PLESSET PERTURBATION CALCULATIONS TO HIGH ORDER

A. Computational details

In this section, we report perturbation calculations on CH_2 , BH, Ne, F^- , and HF. The calculations were carried out at the equilibrium geometries given in Ref. 4, except for BH, where we used $R_{\text{BH}} = 2.3289a_0$. For HF, additional calculations were carried out at the stretched geometry $2.5R_{\text{HF}}$,

where $R_{\text{HF}} = 0.91694 \text{ \AA}$. For CH_2 , BH, Ne, and F^- , the calculations were carried out in the aug-cc-pVDZ basis¹⁵ (unless otherwise specified). For HF, the calculations were carried out using the cc-pVDZ¹⁶ basis and the aug-cc-pVDZ basis with the diffuse p functions on hydrogen and the diffuse d functions on fluorine removed (aug'-cc-pVDZ). In all calculations, only the valence electrons were correlated. The LUCIA program^{17,18} was used for the perturbation calculations.

B. CH_2 : An example of molecules containing low-lying double excited states

Many molecules have low-lying doubly-excited states of the same spin and spatial symmetry as the ground state. For such molecules, the ground-state wave functions typically have a significant contribution from the doubly excited configuration—that is, from the zeroth-order low-lying excited state. Examples of small molecules with such near-degeneracies are CH_2 , BH, and C_2 . In this section, we discuss the convergence of Møller–Plesset perturbation theory for such molecules, using as an example CH_2 and commenting briefly on BH.

Since the single-reference wave function is a poor approximation to the ground state, one would expect the MP expansion of these systems to diverge. However, using a DZP basis for carbon and a DZ basis for hydrogen, Knowles *et al.*⁶ found no indication of divergence in the first ten energy corrections for CH_2 . In Table II, we have listed the first 50 energy corrections for the CH_2 molecule in the aug-cc-pVDZ basis. All corrections are negative. In Fig. 1, the magnitudes of the energy corrections have been plotted on a logarithmic scale (upper curve). From Table II, we obtain a ratio of 0.78 between two consecutive corrections.

Although the expansion in Fig. 1 looks convergent, convergence can only be established by locating the points of

TABLE II. Møller–Plesset energy corrections (in mE_h) for CH_2 using the aug-cc-pVDZ basis.

Order n	$E^{(n)}$	Order n	$E^{(n)}$
1	-18 570.021 18	26	-0.003 953 7
2	-115.682 368 0	27	-0.003 137 5
3	-21.138 383 3	28	-0.002 485 4
4	-6.312 700 6	29	-0.001 965 2
5	-2.145 142 3	30	-0.001 550 8
6	-1.007 196 8	31	-0.001 221 2
7	-0.546 686 1	32	-0.000 959 6
8	-0.350 448 1	33	-0.000 752 2
9	-0.237 962 0	34	-0.000 588 2
10	-0.173 083 5	35	-0.000 458 7
11	-0.128 876 6	36	-0.000 356 7
12	-0.098 823 4	37	-0.000 276 6
13	-0.076 621 8	38	-0.000 213 7
14	-0.060 211 2	39	-0.000 164 6
15	-0.047 572 6	40	-0.000 126 2
16	-0.037 818 0	41	-0.000 096 4
17	-0.030 133 8	42	-0.000 073 3
18	-0.024 070 1	43	-0.000 055 4
19	-0.019 237 3	44	-0.000 041 6
20	-0.015 383 0	45	-0.000 031 1
21	-0.012 295 3	46	-0.000 023 0
22	-0.009 822 4	47	-0.000 016 9
23	-0.007 838 6	48	-0.000 012 2
24	-0.006 248 6	49	-0.000 008 8
25	-0.004 974 1	50	-0.000 006 2

degeneracy of $\mathbf{H}(z)$. For molecules such as CH_2 , the low-lying doubly excited state is the most obvious candidate for an intruder and it is thus appropriate to use this state and the physical ground state as the basis vectors for a two-dimensional subspace. Diagonalizing the zeroth-order Hamiltonian in the subspace spanned by the two wave functions, we obtain the zeroth-order and full Hamiltonians,

$$\mathbf{H}_0 = \begin{pmatrix} -20.089\,28 & 0.0 \\ 0.0 & -19.169\,61 \end{pmatrix}, \quad (23)$$

$$\mathbf{H} = \begin{pmatrix} -39.018\,42 & -0.028\,56 \\ -0.028\,56 & -38.855\,50 \end{pmatrix}, \quad (24)$$

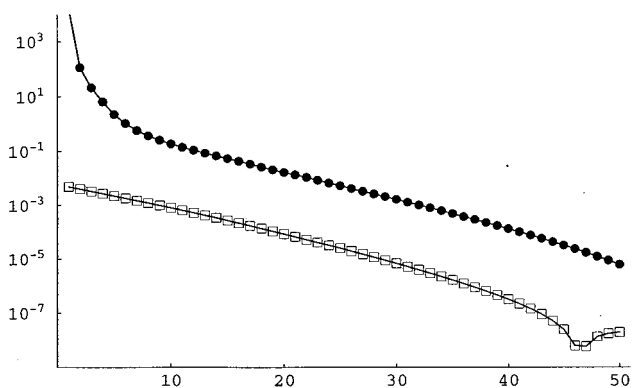


FIG. 1. The absolute values of the perturbation corrections for CH_2 in the aug-cc-pVDZ basis (upper curve) and from the two state representation using the parameters in Eqs. (25)–(27) (lower curve).

which gives the parameters

$$\epsilon = 0.162\,92, \quad (25)$$

$$\gamma = 0.756\,76, \quad (26)$$

$$\delta = 0.028\,559, \quad (27)$$

where we have chosen the phase of the two eigenvectors such that δ is positive. Using Eq. (13), the point of degeneracy for this two-state problem becomes

$$\zeta_{\pm} = 1.208\,40 \pm 0.091\,20i. \quad (28)$$

Since this point lies outside the unit circle, the low-lying doubly excited state is not an intruder. Indeed, a more elaborate search for avoided crossings for $z > 0$ reveals an avoided crossing at $z = 1.2$.

Even though the presence of the doubly excited state does not lead to divergence, it does explain the slow convergence of the expansion. To see this, consider the perturbation expansion in the above two-dimensional subspace. From Eqs. (26)–(27), we see that the gap shift is significantly larger than the coupling element. We may therefore use Eq. (21) for the energy corrections. Accordingly, we predict the ratio between consecutive energy corrections using Eq. (22) as

$$\frac{E^{(n)}}{E^{(n-1)}} = 0.82, \quad (29)$$

in good agreement with the observed ratio of about 0.78. Thus, the first 40 corrections for CH_2 decrease only slowly in magnitude—not because of a large coupling between the ground state and the doubly excited state but because the zeroth-order Hamiltonian severely overestimates the energy gap between the two states.

In Fig. 1, the lower curve is a plot of the absolute values of the energy corrections of the two-state problem. The energy corrections obtained from the two-state problem are several orders of magnitude smaller than those obtained from the full expansion. This is to be expected since the two-state problem includes only the interaction between the two lowest states. The large contributions to the energy corrections from dynamic correlation are therefore absent in the two state model.

The two curves in Fig. 1 are nearly linear, with similar curvatures for orders 10–40, substantiating the notion that the convergence of the full perturbation expansion is closely related to the lowest doubly excited state. For orders less than 10, the full perturbation expansion contains significant contributions from states other than the lowest doubly excited state; for orders higher than 40, the two-state model and the full expansion both deviate from linearity. This behavior is not in conflict with the two-state model itself; it merely shows that the one-term approximation, Eq. (22), is poor for higher orders. In the two-state model, the energy corrections change sign and are positive for orders 52–93. A similar behavior is expected for the full energy corrections.

For the BH molecule in the aug-cc-pVDZ basis, a similar analysis shows that there are no front-door intruders for this system as well. For the two-state model spanned by the ground state and by the low-lying doubly excited state, the

TABLE III. Møller–Plesset energy corrections (in mE_h) for neon using the aug-cc-pVDZ and the aug-cc-pVTZ' basis sets.

Order n	$E_{\text{aug-cc-pVDZ}}^{(n)}$	$E_{\text{aug-cc-pVTZ}'}^{(n)}$
1	-53 907.365 36	-25 709.612 50
2	-206.873 508 5	-244.690 266 7
3	-1.547 443 3	1.719 475 4
4	-5.686 207 4	-7.469 483 4
5	2.013 699 1	2.000 452 8
6	-1.582 384 8	-1.494 566 5
7	0.959 125 5	0.898 918 6
8	-0.707 420 7	-0.674 272 6
9	0.537 928 8	0.513 454 2
10	-0.439 802 3	-0.416 984 0
11	0.375 500 2	0.351 804 8
12	-0.334 462 8	-0.309 001 1
13	0.308 421 4	0.281 169 5
14	-0.293 243 4	-0.264 390 8
15	0.286 368 6	0.256 220 8
16	-0.286 354 9	-0.255 288 3
17	0.292 429 4	0.260 941 4
18	-0.304 288 5	-0.273 074 0
19	0.321 979 6	0.292 042 6
20	-0.345 841 3	-0.318 645 1
21	0.376 478 2	0.354 148 1
22	-0.414 758 7	-0.400 358 2
23	0.461 831 4	0.459 738 3
24	-0.519 155 9	-0.535 576 3
25	0.588 548 1	0.632 217 2

zeroth-order Hamiltonian again overestimates the energy difference between the two lowest states, leading to a positive gap shift that is large compared with the coupling element. Again, the large gap shift leads to slow convergence. For the BH molecule, the point of degeneracy in the space spanned by the two lowest FCI wave functions gives $\zeta_{\pm} = 1.41 \pm 0.19i$.

Obviously, our analysis of the convergence for CH_2 and BH does not eliminate the possibility that these sequences may ultimately diverge because of back-door intruders. We shall now consider such intruder states.

C. Ne: An example of a back-door intruder

For systems like the neon atom and the HF molecule, the Møller–Plesset expansion diverges, with the onset of divergence between orders 10 and 20.⁴ In this section, we study the back-door intruders responsible for this divergence, demonstrating that the divergence is a consequence of the choice of the zeroth-order operator. Our example will be the neon atom in the aug-cc-pVDZ basis.

Table III contains (in the second column) the Møller–Plesset energy corrections up to order 25. In Fig. 2, we present information about the lowest FCI eigenvector of $\mathbf{H}(z)$ of symmetry 1S for real z : the upper panel contains the energy difference between the two lowest 1S states, the middle panel the weight of the Hartree–Fock configuration in the lowest state, and the lower panel the expectation value of r^2 (measuring the diffuseness of the lowest state). We observe an avoided crossing at about $z = -0.82$ —for $z < -0.82$, the wave function of the lowest energy has only a

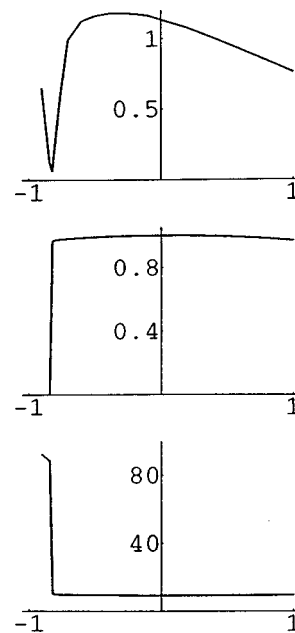


FIG. 2. Information from an energy scan on the real axis for Ne in the aug-cc-pVDZ basis. The upper panel contains the energy difference between the two lowest 1S states, the middle panel gives the weight of the Hartree–Fock configuration in the lowest state, and the lowest panel gives the expectation value of r^2 .

very small component of the ground-state configuration and is very diffuse.⁵

The intruder state is observed also in restricted scans, where the avoided crossing is studied in the subspace of the correction vectors, as previously discussed. In Fig. 3, we give the difference between the two lowest eigenvalues of $\mathbf{H}(z)$ for the subspaces containing the correction vectors up to orders n equal to 2, 4, 6, 8, and 10, respectively, with the scan extended to the interval $[-2, 2]$. For $n=2$, there is no indication of a back-door intruder; for $n>2$, there is a pronounced avoided crossing that moves toward the origin with increasing n . For $n=4$, the avoided crossing is clearly outside the unit circle; for $n=6$, it is close to the unit circle. Finally, in the highest-order subspaces ($n=8, 10$), the

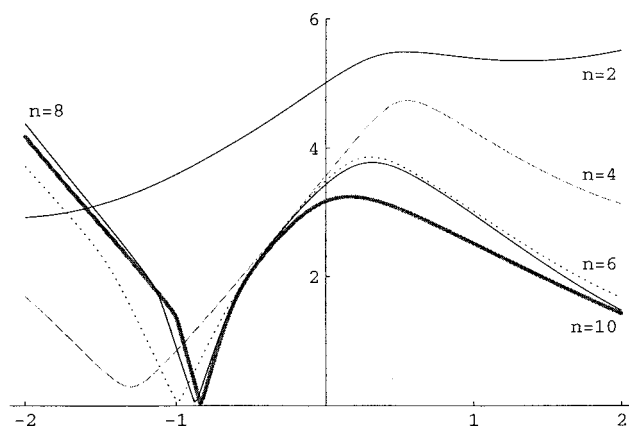


FIG. 3. The energy difference in calculations on Ne using the aug-cc-pVDZ basis between the two lowest eigenvalues of $\mathbf{H}(z)$ for the subspaces containing the correction vectors up to orders n equal to 2, 4, 6, 8, and 10, respectively.

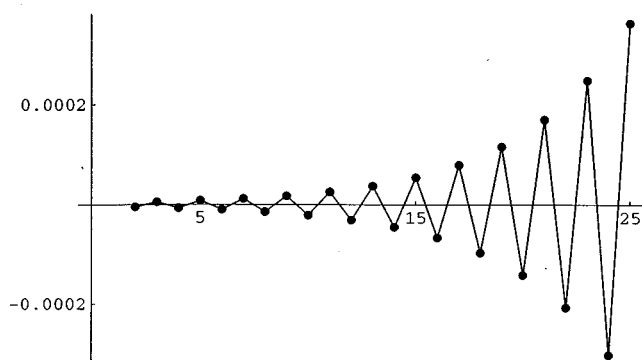


FIG. 4. The energy corrections for Ne in the two-state model using the parameters in Eqs. (32)–(34).

avoided crossing is located inside the unit circle close to $z = -0.82$ —the location obtained from the energy scan.

To investigate the intruder state in more detail, we study the two-state problem spanned by the two lowest states at $z = -0.82$. In the basis of the vectors that diagonalize \mathbf{H}_0 in this subspace, we obtain

$$\mathbf{H}_0 = \begin{pmatrix} -74.43285 & 0.0 \\ 0.0 & -66.87413 \end{pmatrix}, \quad (30)$$

$$\mathbf{H} = \begin{pmatrix} -127.9758 & 0.0059 \\ 0.0059 & -111.2763 \end{pmatrix}. \quad (31)$$

In the following, we shall refer to the higher state as the intruder state (*i*) and to the lower state as the ground state (*g*). From the above matrices, we obtain the parameters

$$\epsilon = 16.6995, \quad (32)$$

$$\gamma = -9.14078, \quad (33)$$

$$\delta = 0.0059. \quad (34)$$

These parameters predict the point of degeneracy,

$$\zeta_{\pm} = -0.827 \pm 0.001i, \quad (35)$$

showing that there indeed is a point of degeneracy within the unit circle—that is, an intruder state. Since the coupling is small compared with the gap shift, we can invoke Eq. (21) to explain the alternating sign of the energy corrections.

In Fig. 4, we present the energy corrections for the perturbation expansion as given by the two-state model with the

TABLE IV. Breakdown of wave function into weights of excitation levels for the intruder state of Ne in aug-cc-pVDZ basis.

Excitation level	Weight
8	0.093603
7	0.258588
6	0.350948
5	0.203870
4	0.071053
3	0.017687
2	0.003506
1	0.000705
0	0.000040

TABLE V. Occupation numbers n and expectation values r^2 for natural orbitals of the ground and intruder state for Ne using FCI in the aug-cc-pVDZ basis set.

Orbitals	Ground state		Intruder state	
	n	$r^2/\text{a.u.}$	n	$r^2/\text{a.u.}$
1s	2.000	0.0335	2.000	0.0335
2s	1.991	1.0834	1.971	4.1472
2p _x , 2p _y , 2p _z	1.979	1.2695	1.993	13.135

parameters in Eqs. (32)–(34). Note that, for the two-state model, the energy corrections are significantly smaller than the full corrections of Table III.

Expressed in terms of the Hartree–Fock orbitals, the intruder state is a rather complicated wave function. In Table IV, we have analyzed the intruder state in terms of the various excitation levels using the Hartree–Fock orbitals. More than 70% of the weight of the wave function arises from sixfold or higher excitations. In Table V, we give the natural occupation numbers and the expectation values of r^2 for the FCI ground state [obtained as the lowest root of $\mathbf{H}(1)$] and for the intruder state [obtained as the second state that diagonalizes \mathbf{H}_0 in the space spanned by the two lowest roots of $\mathbf{H}(-0.82)$]. The occupation numbers of the intruder state shows that this state is well represented by the single electronic configuration $1s^2 2s'^2 2p'^6$, where the $2s'$ and $2p'$ orbitals are very diffuse and differ significantly from the canonical orbitals of the ground-state Hartree–Fock configuration.

The occurrence of the highly diffuse back-door intruders may be explained using simple physical arguments. We first note that the zeroth- and first-order energies are usually several orders of magnitude larger than the higher-order corrections. The energy of a state k can therefore be accurately approximated by the linear form

$$E_k^l(z) = E_k^{(0)} + zE_k^{(1)}. \quad (36)$$

In Fig. 5, we have used this approximation for the ground state and for the intruder state of the two-state problem. The zeroth- and first-order energies have been extracted from the

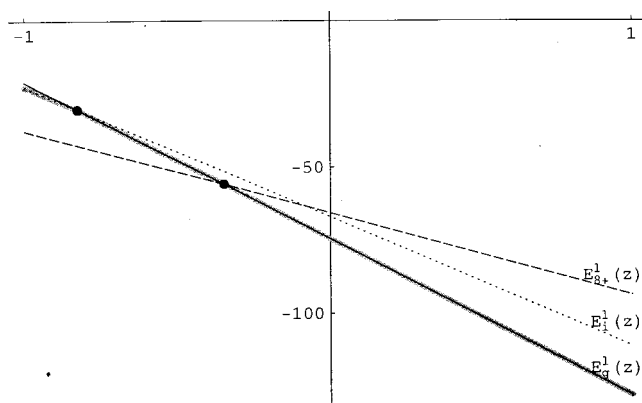


FIG. 5. The total energies $E_g(z)$ (gray line), $E_g^l(z)$ (thin full line), $E_i^l(z)$ (dotted line), and $E_{g+}^l(z)$ (dashed line) as a function of z .

diagonal elements of the matrices \mathbf{H}_0 and \mathbf{H} of Eqs. (30)–(31), leading to the following linear expressions for the energies of the ground and intruder states:

$$E_g^l(z) = -74.43285 - 53.54295z, \quad (37)$$

$$E_i^l(z) = -66.87413 - 44.40217z. \quad (38)$$

Figure 5 also contains the true energy function $E_g(z)$, obtained as the lowest eigenvalue of $\mathbf{H}(z)$. The curves of the energy functions $E_g^l(z)$ and $E_g(z)$ are very nearly identical, demonstrating the validity of the linear approximation.

Although the intruder state is high above the ground state for $z \geq 0$, their different slopes give rise to a crossing for $z < 0$. The linear approximation predicts a crossing for $z = -0.827$, which agrees well with the true location of degeneracy. The curve crossing is thus a consequence of the presence of states that, compared with the ground state, have a significantly higher zeroth-order energy but a significantly smaller absolute value of the first-order energy. In Møller–Plesset perturbation theory, the first-order energy is equal to the electron-repulsion energy of the reference determinant. Configurations with very diffuse electron distributions will thus necessarily have a numerically small first-order energy correction.

The above divergence of the Møller–Plesset expansion is thus caused by crossings of the ground-state energy curve with the curves of states that, for the physical Hamiltonian, are located high in the continuum. To illustrate this point, we have in Fig. 5 also given the linear energy approximation,

$$E_{8+}^l = E_{8+}^{(0)} + E_{8+}^{(1)}z = -65.5899 - 28.2590z, \quad (39)$$

for a hypothetical neon state containing the two $1s$ electrons and with the eight valence electrons located so far away from the nucleus that the system can be considered a Ne^{8+} ion. The zeroth- and first-order energies of this ion have been obtained from the \mathbf{H}_0 and \mathbf{H} operator of the neutral atom in the aug-cc-pVDZ basis. The ground-state curve is predicted to cross the curve for the ionized atom for $z = -0.35$. As the basis increases, states similar to this ionized state will be included and lead to avoided crossings in this region.

The identification of back-door intruders as diffuse continuum states explains a number of puzzling features in the observed divergences. First, it is now clear why the divergences are observed only when diffuse functions are added since only then are continuum states of low electron repulsion present. Second, the back-door intruders are very highly excited since all valence orbitals change from contracted to diffuse orbitals. Third, the divergences are more pronounced for electron-rich systems such as neon: For such systems, the first-order energy is numerically large with the result that $E_g(z)$ rises sharply into the continuum for $z < 0$, increasing the likelihood of crossings for $z > -1$.

According to this discussion, an increase of the basis should not remove the intruder states even if only contracted functions are added. As an illustration, we have listed in the third column of Table III the energy corrections obtained by using the truncated aug-cc-pVTZ' basis, obtained from the aug-cc-pVTZ basis by removing the f functions. The energy

corrections of the aug-cc-pVDZ and the truncated aug-cc-pVTZ' basis are very similar and the divergence is equally pronounced in the two cases.

The validity of the above discussion of divergence due to diffuse back-door intruders is not restricted to the neon atom. We have investigated a number of other atoms and molecules with high electron densities and many interacting electrons and observed similar crossings of the ground state and the continuum states for negative z . In the next section, we shall discuss HF. Here, we comment briefly on the intruder states for the anion F^- .

As described previously,⁴ the F^- system diverges already from third order. A scan of the spectrum of $\mathbf{H}(z)$ shows an avoided crossing at $z = -0.64$. In a subspace spanned by the two lowest 1S roots of $\mathbf{H}(-0.64)$ and in the basis that diagonalizes the zeroth-order Hamiltonian in this subspace, we obtain a coupling element of 0.047. This coupling is significantly larger than the corresponding coupling in neon, explaining the more rapid divergence in F^- .

For the less electron-rich molecules, back-door intruder states may be observed in extended basis sets. For the BH molecule, there are no back-door intruders in the aug-cc-pVDZ and d-aug-cc-pVDZ basis sets. However, in the t-aug-cc-pVTZ basis, we may identify a back-door intruder with $\zeta_{\pm} = -0.98 \pm 5 \times 10^{-8}i$. However, because of the very small coupling and the proximity of the critical ζ to the unit circle, no signs of this intruder are detected in the first 50 terms of the Møller–Plesset expansion. As the energy corrections after the first 50 terms are smaller than 10^{-12} , we may regard this BH expansion to be practically converged. However, if the expansion is continued beyond order 50, the divergence must eventually occur.

For the CH_2 molecule, there are no intruders in the aug-cc-pVDZ basis. When a second set of diffuse functions is added at the d-aug-cc-pVDZ level, we observe a back-door intruder. Again, the perturbation expansion can be continued to a convergence of 10^{-10} with no sign of divergence. For these molecules where intruder states show up only when two or three sets of diffuse functions are added, the coupling to the reference state is so small that, for all practical purposes, the intruders do not affect the convergence of the expansion.

The question of convergence or divergence of perturbation expansions was above analyzed using the FCI states obtained by diagonalizing $\mathbf{H}(z)$. However, an examination of the zeroth- and first-order energy corrections of the different configurations is usually sufficient to answer the question of convergence. We shall discuss this point in a separate communication.

D. HF: Examples of calculations containing both back-door intruders and low-lying excited states

We first consider calculations on HF at the equilibrium geometry R_{HF} in the cc-pVDZ basis. In Fig. 6, we have plotted information about the lowest two roots of $\mathbf{H}(z)$ for this system. The upper plot contains the energy of the lowest state, the second plot contains the difference between the energies of the two lowest roots, the third plot contains the coefficient of the ground-state determinant for the lowest

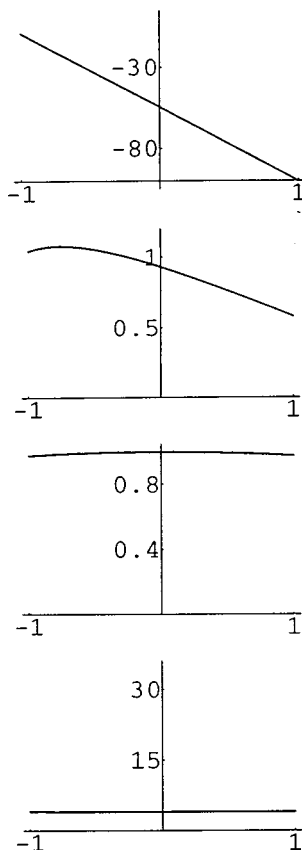


FIG. 6. Information from an energy scan on the real axis for HF at equilibrium geometry in the cc-pVDZ basis. The upper panel contains the energy of the lowest state, the second panel contains the energy difference between the two lowest states, the third panel gives the coefficient of the Hartree-Fock configuration in the lowest state, and the lowest panel gives the expectation value of x^2 .

root, and the fourth and lowest plot gives the expectation value of x^2 for the lowest root. The x axis is orthogonal to the molecular axis and the expectation value of x^2 measures the diffuseness of the state. No avoided crossings are observed in the interval $z = [-1, 1]$: there is no minimum in the excitation-energy curve and the ground-state wave function is dominated by the Hartree-Fock determinant for all z . Consequently, we expect the Møller-Plesset expansion to converge, as confirmed by the Møller-Plesset energy corrections plotted in Fig. 7.

Adding the diffuse functions to the basis at the equilibrium geometry, we obtain the scan in Fig. 8. There is now a pronounced avoided crossing at $z = -0.743$. The shape of the energy-difference curve (i.e., the near-degeneracy of the energies and the absence of interaction when z is slightly larger than -0.743) indicates that the coupling between the ground state and the intruder state is very small. To quantify the coupling and the gap shift, calculations were performed in the subspace of the two lowest $^1\Sigma$ states of $\mathbf{H}(-0.743)$. In this subspace, the zeroth-order states give the matrices

$$\mathbf{H}_0 = \begin{pmatrix} -54.65980 & 0.00000 \\ 0.00000 & -49.41060 \end{pmatrix}, \quad (40)$$

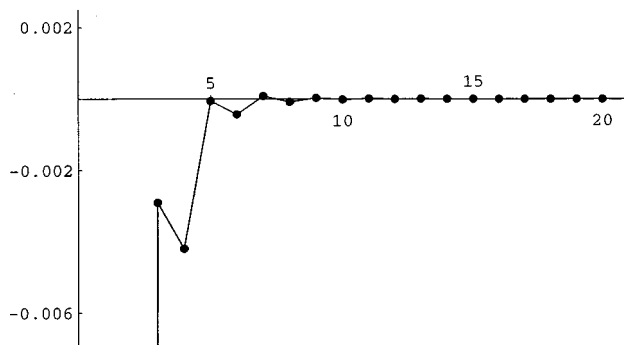


FIG. 7. The energy corrections for HF at equilibrium geometry in the cc-pVDZ basis.

$$\mathbf{U} = \begin{pmatrix} -44.91005 & 0.00034 \\ 0.00034 & -37.84247 \end{pmatrix}, \quad (41)$$

which correspond to

$$\epsilon = 12.31678, \quad (42)$$

$$\gamma = -7.06758, \quad (43)$$

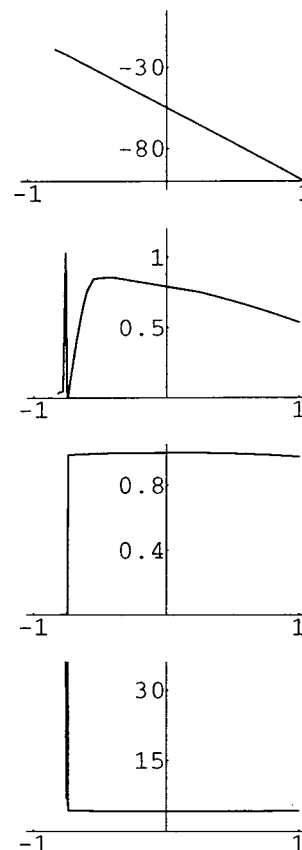


FIG. 8. Information from an energy scan on the real axis for HF at the equilibrium geometry in the aug'-cc-pVDZ basis. The upper panel contains the energy of the lowest state, the second panel contains the energy difference between the two lowest states, the third panel gives the coefficient of the Hartree-Fock configuration in the lowest state, and the lowest panel gives the expectation value of x^2 .

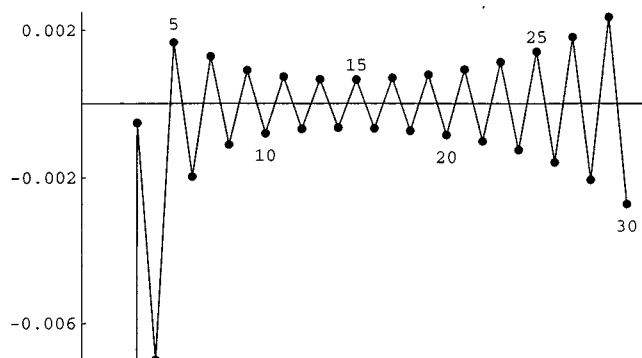


FIG. 9. The energy corrections for HF at equilibrium geometry in the aug'-cc-pVDZ basis.

$$\delta = 0.000\ 34. \quad (44)$$

The coupling element is indeed small. The weak coupling arises since the intruder is dominated by quadruple and higher excitations into the diffuse functions. The predomination of excitations into diffuse orbitals is reflected in the expectation value of x^2 , which changes abruptly at the avoided crossing. The location of the crossing may again be estimated from linear expansions of the energies of the ground state and the intruder state. Obtaining the zeroth- and first-order energies from Eqs. (40) and (41), we predict an avoided crossing at $z = -0.743$, in perfect agreement with the value obtained from the energy scan.

The Møller–Plesset expansion for HF is thus divergent in the aug-cc-pVDZ basis. The divergence is clearly seen in Fig. 9, where we have plotted the Møller–Plesset energy corrections for this system. The sign of the energy corrections alternate, as predicted from Eq. (21).

Turning next to the results for the stretched bond, we give in Fig. 10 the results of the scan in the cc-pVDZ basis. In the energy-difference curve, we observe two avoided crossings: a shallow minimum at $z = 0.8$ and a sharp minimum at $z = -0.598$. We shall investigate these avoided crossings separately, using the two-state model.

For the avoided crossing at $z = 0.8$, the two-state Hamiltonian is defined by the matrices

$$\mathbf{H}_0 = \begin{pmatrix} -56.374\ 951 & 0.000\ 00 \\ 0.000\ 00 & -55.974\ 842 \end{pmatrix}, \quad (45)$$

$$\mathbf{U} = \begin{pmatrix} -43.565\ 86 & 0.1195 \\ 0.1195 & -43.878\ 70 \end{pmatrix}, \quad (46)$$

which give

$$\epsilon = 0.087\ 27, \quad (47)$$

$$\gamma = 0.3128, \quad (48)$$

$$\delta = 0.1195. \quad (49)$$

The points of degeneracy are obtained from Eq. (13) as $\zeta_{\pm} = 0.80 \pm 0.62i$. The relatively strong coupling is consistent with the large separation between the curves at the avoided crossing. The point of degeneracy is predicted to be just outside the unit circle. In general, when a point of degeneracy z^* having a significant imaginary component is close

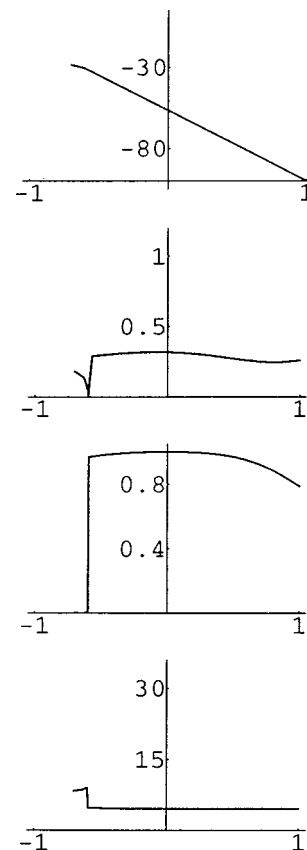


FIG. 10. Information from an energy scan on the real axis for HF at the stretched geometry in the cc-pVDZ basis. The upper panel contains the energy of the lowest state, the second panel contains the energy difference between the two lowest states, the third panel gives the coefficient of the Hartree–Fock configuration in the lowest state, and the lowest panel gives the expectation value of x^2 .

to the boundary of the unit circle, it may be necessary to determine the eigenvectors of $\mathbf{H}(z^*)$ in the full CI space to establish whether the point of degeneracy represents an intruder state. As the gap shift and the coupling are of similar magnitude, the simple one-term expansion in Eq. (21) cannot be used. In Fig. 11, we have plotted the perturbation expansion using Eq. (12) with the above obtained values. Although not evident from Fig. 11, the perturbation series is ultimately converging.

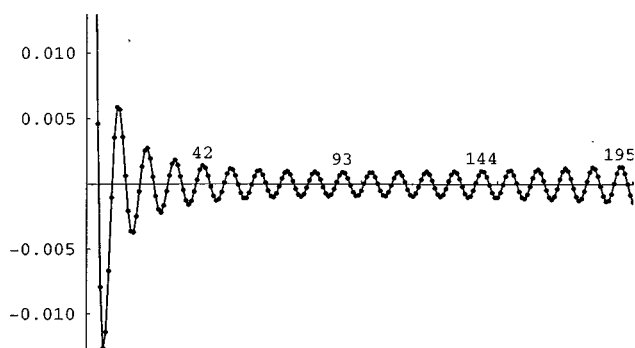


FIG. 11. The energy corrections for HF in the two-state model using the parameters in Eqs. (47)–(49).

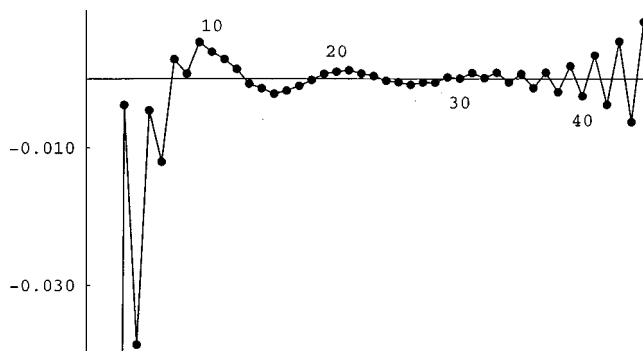


FIG. 12. The energy corrections for HF at stretched geometry in the cc-pVDZ basis.

The avoided crossing at $z = -0.598$ is much more pronounced. Accordingly, the two-state model using the two lowest states of $\mathbf{H}(-0.598)$ gives a sharp crossing at $z = -0.598$. The Hamiltonian matrices of this model are given by

$$\mathbf{H}_0 = \begin{pmatrix} -56.41951 & 0.00000 \\ 0.00000 & -44.29616 \end{pmatrix}, \quad (50)$$

$$\mathbf{U} = \begin{pmatrix} -42.817676 & 2 \times 10^{-8} \\ 2 \times 10^{-8} & -22.54257 \end{pmatrix}, \quad (51)$$

giving a point of degeneracy $\zeta_{\pm} = -0.598 + 1.2 \times 10^{-9}i$, which corresponds to a back-door intruder very close to the real axis.

The dominant contribution to the intruder state may be written as $1\sigma'^2 2\sigma'^2 3\sigma'^2 1\pi'_x 1\pi'_y$, where $2\sigma'$ is the antibonding sigma orbital, $3\sigma'$ the most diffuse hydrogen function, and the π' orbitals consist of the hydrogen p orbitals orthogonal to the molecular axis. Thus, the intruder represents a state with six electrons in the most diffuse hydrogen functions. We also note that the reason for the occurrence of the back-door intruder at the stretched geometry (as opposed to the equilibrium geometry) is not an increased first-order correction—in fact, the first-order ground-state energy is $2.3E_h$ lower at the equilibrium geometry than at the stretched geometry ($-45.4802E_h$ vs $-43.1801E_h$). Rather, the intruder is stabilized by a reduced zeroth-order gap $E_i^{(0)} - E_g^{(0)}$ that arises from a lowering of the virtual orbital energies and a simultaneous raising of the occupied orbital energies. Thus, the antibonding orbital has a negative orbital energy of $-0.12957E_h$ at the stretched geometry, whereas the lowest energy for a totally symmetric virtual orbital at equilibrium is $0.18385E_h$. The intruder state is again stabilized compared to the ground state by a numerically much smaller first-order energy. Within the two-state model, the first-order energy of the intruder state and the ground state is thus $-22.54257E_h$ and $-42.81768E_h$, respectively.

In Fig. 12, we have plotted the MP sequence to order 50. The series behaves in a manner that reflects the presence of both avoided crossings discussed above. Thus, after a few irregular corrections, corrections 10–30 exhibit a slowly undulating pattern that is determined by the interaction with the strongly coupled would-be front-door intruder. For higher orders the interaction with the weakly coupled back-door

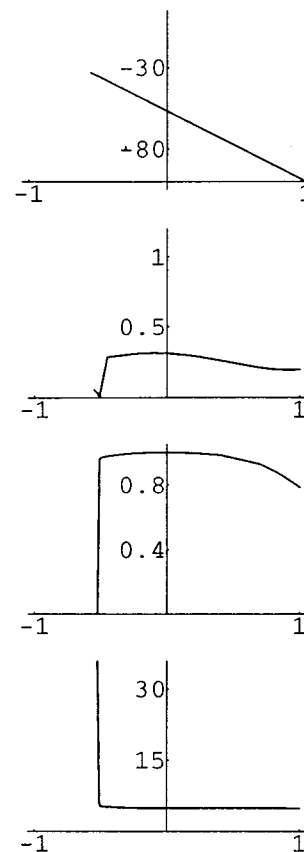


FIG. 13. Information from an energy scan on the real axis for HF at the stretched geometry in the aug'-cc-pVDZ basis. The upper panel contains the energy of the lowest state, the second panel contains the energy difference between the two lowest states, the third panel gives the coefficient of the Hartree-Fock configuration in the lowest state, and the lowest panel gives the expectation value of x^2 .

intruder takes over and the series begins to alternate and diverge in a manner typical of such intruders. Note that, even though the most strongly coupled electronic state governs in lowest order, the fate of the series is eventually determined by the weakly coupled back-door intruder.

The last case to be studied is the HF molecule at the stretched geometry in the diffuse basis. In Fig. 13, we have listed the results of the corresponding scan of $\mathbf{H}(z)$. For positive z , there is a very weak avoided crossing around 0.9 and a pronounced avoided crossing at $z = -0.51$. For the avoided crossing at $z = 0.9$, there is no obvious change of the character of the wave function, whereas the avoided crossing at $z = -0.51$ is associated with abrupt changes of the lowest state: a sharp drop in the weight of the Hartree-Fock determinant and a sudden increase in the diffuseness of the state.

The two-state model reveals that the weak avoided crossing is associated with the points of degeneracy $0.92 \pm 0.53i$, which are sufficiently far removed from the unit circle that we can rule out the possibility of an intruder. Conversely, for the degeneracy at negative z , we obtain from the two-state model [employing the two lowest eigenvectors of $\mathbf{H}(-0.51)$] $\zeta_{\pm} = -0.510 \pm 6 \times 10^{-5}i$, indicating the presence of an intruder. The small imaginary part of the points of degeneracy agrees with the very small energy gap at the avoided crossing. Figure 14 gives the MP series to order 15,

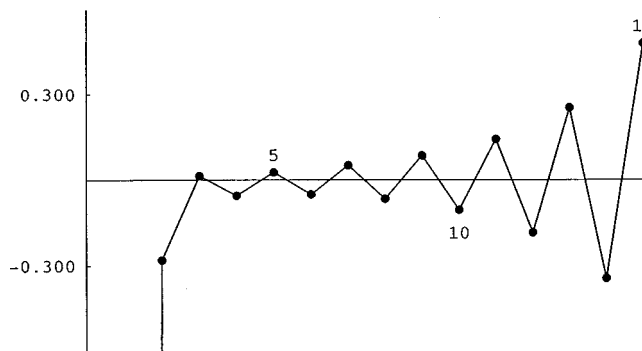


FIG. 14. The energy corrections for HF at stretched geometry in the $\text{aug}'\text{-cc-pVDZ}$ basis.

showing a divergent, alternating series already at third order.

E. Relations between low- and high-order convergence

From perturbation calculations through order 6, Cremer and He² have classified molecules as belonging to either class A or class B. Class A systems have perturbation corrections that are monotonically decreasing while class B systems have perturbation corrections that alternate in sign. In accordance with the previous discussion, class B molecules contains electron-rich atoms whereas class A molecules contain atoms with fewer electrons. Our calculations and analysis show that that it is difficult, and not in general mathematical motivated, to extrapolate from low-order to the asymptotic behavior. In particular, the question of convergence or divergence cannot be determined by a study of the lowest orders energy contributions. An example is HF, which is a class B system with the initial energy corrections alternating in sign. However, in calculations at the stretched geometry with a nonaugmented basis, the perturbation corrections only alternate in sign up to order ten, after which the corrections have the form of a damped sinus function with a period of about 20. From about order 30 the series starts to diverge with perturbation corrections alternating in sign.

F. Alternative partitionings

In the previous discussion, we have restricted our attention to the Møller–Plesset theory. It may be of interest to comment briefly on other partitions. The diagonal of the Hamiltonian in the Slater determinant or configuration state basis is occasionally used as the zeroth-order Hamiltonian leading to the Epstein–Nesbet partitioning. As the first-order energy vanishes trivially for this partitioning, there are, of course, no back-door intruders due to numerically large first-order energies. A scan for HF at the equilibrium distance R_{HF} in the diffuse $\text{aug}'\text{-pVDZ}$ basis shows accordingly no intruderstates. Instead an avoided crossing at $z \approx -1.1$ is observed. This avoided crossing is due to the interaction between the reference state and an excited state dominated by singly and doubly excited configurations. The Epstein–Nesbet perturbation expansion is thus convergent for HF us-

ing the $\text{aug}'\text{-pVDZ}$ basis. If the HF bond is stretched to $2R_{\text{HF}}$, the Epstein–Nesbet perturbation expansion exhibits rapid divergence.

An alternative modification of the Møller–Plesset partitioning is based on the use of modified virtual orbitals. However, in this approach the occupied orbitals are usually not modified, so the energy of the reference state will again rise into the continuum for negative values of z .

IV. CONCLUSIONS

We have demonstrated how the convergence patterns of MP series can be understood in terms of a simple mathematical model, which can be given a simple physical interpretation. The computational complexity of the analysis is much larger than the complexity of solving the FCI problem and thus cannot be used as a practical remedy for a divergent MP series.

For molecules with low-lying double excited states, as CH_2 , BH, and HF at the stretched geometry, we have observed points of degeneracy in the half-plane with a positive real value. For CH_2 , BH, and stretched HF using the $\text{aug}'\text{-cc-pVDZ}$ basis, these points of degeneracy were definitely outside the unit circle. For stretched HF using the cc-pVDZ basis, this point of degeneracy was detected to be just outside the unit circle. Studying the two-state problem in the space spanned by the ground state and the low-lying double excited state, we observe a significant coupling between the two zeroth-order functions, and the zeroth-order energy gap severely overestimates the energy gap. The large coupling element causes the corrections in the initial orders to be large, whereas the large overestimation of the energy gap in zeroth order causes the very slow decrease in the energy corrections. These observations explains the initial slow monotonic convergence of the MP series for these molecules. As the above points of degeneracy all are located outside the unit circle, they do not cause divergence.

All molecules examined in the present paper exhibit back-door intruders in basis sets containing sufficient diffuse functions. For the molecules BH and CH_2 , where the back-door intruders only occur when double or higher augmented basis sets are used, the MP series converge to better than 10^{-12} in energy, and no signs of divergence occur in the lowest 50 orders. Although the MP series in these cases may be considered practically converged, the sequences ultimately diverge.

The divergences of the MP series for the electron-rich molecules are not related to numerical instabilities nor to basis-set artifacts but are rather inherent to the Møller–Plesset partitioning of the Hamiltonian. The divergences can be reproduced using a simple mathematical analysis based on the two-state model. We believe that it is now firmly established that the divergence for even simple systems such as neon and HF are due to highly excited diffuse back-door intruders, that couple only weakly to the ground state. In our earlier study of the divergences, basis sets of double-zeta quality augmented with diffuse functions were considered. The present calculations include basis sets of triple-zeta quality augmented with diffuse functions, and we find the same divergences in these calculations. In short, the divergences

occur whenever the basis contains sufficient flexibility to give a reasonable description of the highly excited, diffuse back-door intruders. As such, divergence is the rule rather than exception in MP theory, which converges only in small basis sets. Even though the inherent divergence of the MP series does not invalidate the use of the highly successful MP2 level of theory, higher-order corrections should always be treated with caution.

ACKNOWLEDGMENT

This work has been supported by the Danish Natural Research Council (Grant No. 9901973).

¹C. Møller and M. S. Plesset, Phys. Rev. **46**, 618 (1934).

²D. Cremer and Z. He, J. Phys. Chem. **100**, 6173 (1996).

³G. Hose, J. Chem. Phys. **84**, 4504 (1986).

⁴J. Olsen, O. Christiansen, H. Koch, and P. Jørgensen, J. Chem. Phys. **105**, 5082 (1996).

⁵O. Christiansen, J. Olsen, H. Koch, P. Jørgensen, and P. Aa. Malmqvist, Chem. Phys. Lett. **261**, 369 (1996).

⁶P. J. Knowles, K. Somasundram, N. C. Handy, and K. Hirao, Chem. Phys. Lett. **113**, 8 (1985).

⁷W. Laidig, G. Fitzgerald, and R. J. Bartlett, Chem. Phys. Lett. **113**, 151 (1985).

⁸T. H. Dunning and K. A. Peterson, J. Chem. Phys. **108**, 4761 (1998).

⁹S. Wilson, K. Jankowski, and J. Paldus, Int. J. Quantum Chem. **28**, 525 (1985).

¹⁰J. P. Finley, R. K. Chaudhuri, and K. F. Freed, J. Chem. Phys. **103**, 4990 (1995).

¹¹T. Kato, *Perturbation Theory for Linear Operators* (Springer-Verlag, Berlin, 1966).

¹²T. H. Schucan and H. Weidenmüller, Ann. Phys. (N.Y.) **73**, 108 (1972).

¹³K. Dietz, C. Schmidt, M. Warken, and B. A. Hess, J. Phys. Chem. B **26**, 1885 (1993).

¹⁴K. Dietz, C. Schmidt, M. Warken, and B. A. Hess, J. Phys. Chem. B **26**, 1897 (1993).

¹⁵R. A. Kendall, T. H. Dunning, and R. J. Harrison, J. Chem. Phys. **96**, 6769 (1992).

¹⁶T. H. Dunning, J. Chem. Phys. **90**, 1007 (1989).

¹⁷LUCIA, a full CI, restricted active space CI program by J. Olsen Århus with contributions from H. Larsen and M. Fülcher.

¹⁸J. Olsen, B. O. Roos, P. Jørgensen, and H. J. Aa. Jensen, J. Chem. Phys. **89**, 2185 (1988).